Journal of Nondestructive Evaluation (2025) 44:26
https://doi.org/10.1007/s10921-025-01165-1

Acceptance Criteria for Defects in Polyethylene Welds, Coupling Phased Array Ultrasonic Testing and Destructive Tests

Dominique Gueugnaut[1] · Manuel Tessier[2] · Myriam Bechrouri[1] · Aymeric Lopitaux[1]

Received: 1 August 2024 / Accepted: 14 January 2025

Abstract

As a promising reference technique for non-destructive evaluation of both electrowelded and butt-fused polyethylene (PE) assemblies, Phased Array Ultrasonic Testing (PAUT) is still studied extensively in several laboratories worldwide and is supported by the technical standard ISO TS 16943. During the last 10 years, several joint projects have been completed aiming at evaluating the acuity of PAUT applied to both pipes and electrofused assemblies either exhumed from the field or prepared in laboratory. More recently, a focus has been made on fixing some acceptance criteria combining PAUT data and long term resistance of the laboratory joints. This paper presents the updated data obtained on electrofused assemblies—63 mm saddles and 110 mm sockets—containing different types of defects such as: insufficient heating time, pipe under-penetration in the socket, excessive localized scraping, pollutants and calibrated thin strips, in both mass and cross configuration, put at the interface pipe-saddle. PAUT scanning on the different specimens, both during the welding phase and after cooling, confirms the capability of the technique to visualize and size the Heat Affected Zone (HAZ), which can be revealed and compared afterwards on sample sections. Moreover, most of the defects are detected and sized, confirming the fairly good performance of PAUT, except for the smallest strips which are located in non accessible zones, due to the particular design of the saddle. Long term resistance of the welds is then evaluated by Hydrostatic Pressure Tests (HPT) followed by a decohesion test after rupture, according to the requirements of both the ISO 13956 and NF EN 1555 standards. Under such test conditions, every joints comply with the requirements of the standards (rupture time greater than 1000 h at 80 °C and 5 MPa), even those violating the critical proportions of non-welded zones.

Keywords Polyethylene (PE) · Electrofusion · Phased array ultrasonic testing · Heat affected zone · Hydrostatic pressure test · Acceptance criteria

1 Introduction

For over 20 years now, the non-destructive evaluation technique of Phased Array Ultrasonic Testing or PAUT has been extensively assessed by several international institutes and laboratories for polyethylene (PE) welded assemblies, mainly regarding butt-welding and, more recently, electrofusion welding. There has been a particular focus on assemblies with diameters greater than 160 mm, used notably in the context of pressurized mains for water distribution. This technique along with the typology of defects likely to be detected are described in the technical document ISO TS 16943: 2023 [1–24].

Concerning the range of diameters smaller than 160 mm, and more specifically up to the DN110 used in the gas distribution context, studies remain more sparsely documented. To fill this gap, studies have been undertaken by RICE in collaboration with Institut de Soudure Industries to address both the case of welded assemblies and that of single pipes. As a first step, the capabilities of the PAUT technique, in terms of detection and localization of existing surface and volume defects, as well as in terms of defect sizing, have been successfully assessed [8, 19–23].

Regarding electro-welded assemblies specifically, the influence of the presence of surface defects on mechanical strength has been examined by trying to establish a correlation between PAUT results and the destructive decohesion test on DN63 tapping saddle assemblies. In the same vein,

✉ Dominique Gueugnaut
dominique.gueugnaut@grtgaz.com

1 GRTgaz Research & Innovation Center for Energy, F-92390 Villeneuve-la-Garenne, France

2 Institut de Soudure Industrie, F-93420 Villepinte, France

the study of the influence of volume defects (of the "pit" type) introduced in the body of the DN63 tapping tee from its interface has been initiated through hydrostatic pressure tests, more representative of the long-term behavior.

At this stage, the poor sensitivity of the mechanical tests made it difficult to establish a reliable relationship between the energy required to achieve decohesion of the assemblies or the rupture time under hydrostatic pressure test—in view of the small number of tests—and the distribution and proportion of the disorders [25–30].

Consequently, acceptance criteria for defects in PE welded assemblies still need to be determined and it will require establishing strong correlations between the non-destructive PAUT technique and destructive mechanical tests capable of accounting for long-term behaviors. To date, an extremely limited number of relevant studies have been published on the subject and it remains the focus of ongoing discussions [31–37].

To do so, an experimental program which involves both OD63 × 20 mm tapping saddles and OD110 mm diameter couplers with artificial flaws has been designed.

Artificial surface defects are introduced beforehand at the welding interface, either by limiting the heating time compared to the nominal time recommended by the manufacturer, or by sticking thin strips distributed in two ways—referred to as mass- and crossing distributions—across the heating plane of the tapping tees, or by applying a liquid contaminant. Regarding the assemblies using couplers, implementation defects are deliberately re-created, namely: application of a liquid contaminant, incomplete insertion into one of the two sockets of the fitting, and excessive scraping of the pipe through the creation of four facets at a 90° angle in one of the sleeve's two sockets.

All the assemblies are subjected to PAUT control during the welding phase and after cooling, to detect and size both the heat affected zones at the interface (HAZ), and the defects present in the assembly. Hydrostatic pressure tests followed by decohesion tests are subsequently performed to account for the harmful impact of the induced defects on the mechanical performances of the assemblies tested.

For some configurations with the couplers, the Total Focusing Method (TFM) and the Radiographic Technique were also used to compare their sensitivity regarding PAUT. The principles of these three techniques are shortly reminded below.

Phased Array Ultrasonic Testing (PAUT) is an advanced nondestructive examination technique that utilizes a set of ultrasonic testing (UT) probes made up of numerous small elements, each of which is pulsed individually with computer-calculated timing ("phasing"). When these elements are excited using different time delays, the beams can be steered at different angles, focused at different depths, or multiplexed over the length of a long array, creating the electronic movement of the beam. PAUT electronic system using delay laws allowed to generate several types of scans: Linear scan (movement of the acoustic beam along the multi-element probe axis), Sectorial scan (Ability to deflect the acoustic beam at different angles) and Depth focusing scan (beam focusing at different depths).

Total Focusing method (TFM)/Full Matrix Capture (FMC) are recent technological advancements in phased array testing. Full Matrix Capture (FMC) is a data-acquisition process where each array element is sequentially used as a single emitter and all array elements are used as receivers creating a matrix of A-Scan data. FMC has the advantage of acquiring high amounts of data that may be reused later in many ways. Once the data of this matrix is collected, the signal is processed using the Total Focusing Method (TFM) to produce an image (or frame) where each pixel is one dedicated and focused focal law in the region of interest. TFM algorithm is applied to FMC dataset in post processing. Algorithm coherently summing all the signals sij(t) from the dataset to focus at every points of a Region Of Interest (ROI) in a specimen. TFM is particularly useful for reconstructing the data for defect characterization with very good accuracy, but data file sizes are orders of magnitude larger than PAUT.

Radiographic Testing (RT) is a non-destructive testing (NDT) method which uses either X-rays or Gamma-rays to examine the internal structure of manufactured components identifying any flaws or defects. In Radiography Testing the test-part is placed between the radiation source and film (or detector). The material density and thickness differences of the test-part will attenuate the penetrating radiation through interaction processes involving scattering and/or absorption. The differences in absorption are then recorded on film(s) or through an electronic means. This technique shows some limitations in detecting and sizing small defects.

2 Implementation of the Electro-Welded Assemblies

2.1 PE Components

Information regarding the electrofusion fittings and the pipes used in this study is listed in Table 1.

2.2 Electro-Welded Assemblies

48 different OD63 mm pipe_saddles assemblies were distributed as follows:

- 15 assemblies with varying heating times, ranging from 55 to 120% of the nominal heating time specified by the fitting manufacturer.

Table 1 Data pertaining to the electrofusion fittings and the pipes used

PE component	Batch number	Date of manufacture	Lab ID
Tapping saddle OD 63x20 mm	212100	05/2021	16061
Coupler OD110 mm	210300	08/2021	16059
Pipe OD 63 mm SDR11	GA151/01	01/2022	16105
Pipe OD 110 mm SDR11	GA152/02	01/2022	16106

- 15 assemblies with prior insertion of strips simulating the presence of "mass" defects before welding. The strips—-constituted of stickers used generally as optical targets for tensile tests—are around 0.2 mm thick, 5 mm wide, with a length ranging between 5 and 15 mm, with their greatest length oriented parallel to the crown materialized by the heating zone. The surface proportion of the defect relative to that of the fusion zone ranges between 5% and 27.3%, thus lying both below and above the 25% maximum requirement of the ISO 13956 standard dealing with decohesion tests on tapping saddles [26]. In this configuration, the crossing width of the strips accounts for between 22 and 23% of the heating zone of the saddle.
- 15 assemblies with the insertion of strips simulating the presence of "crossing" defects, with their greatest length oriented perpendicular to the crown materialized by the heating zone; The strips are 5 mm wide, with a length ranging between 3 and 14 mm. The percentage represented by the defect lengths relative to the width of the heating zone ranges between 13 and 64%, there again to ensure that the defects are below and above the 50% maximum threshold required by the ISO 13956 standard [26]. In this configuration, the surface distribution of the strips represents between 1.8 and 6.4% of that of the heating zone of the tapping saddle. Figure 1 provides an illustration of the distribution of the strips in the so-called mass and crossing configuration.
- 3 assemblies with liquid contamination of the fusion zone prior to welding. Contamination was carried out by applying a silicone-based liquid spray, followed by very superficial cleaning using a pre-impregnated wipe (Fig. 2).

Among these 48 assemblies, 16 were devoted to HAZ measurement.

24 different OD110 mm pipe_coupler assemblies were designed as follows:

- 15 assemblies with varying heating times, ranging from 55 to 120% of the heating time specified by the fitting manufacturer.
- 3 assemblies with incomplete insertion of a pipe in one of the sockets of the coupler, as illustrated in Fig. 3a.

Table 2 Equipment used for the PAUT control of the tapping saddles and couplers assemblies

Setup	Fitting to be controlled	
	Tapping saddle OD 63x20 mm	Coupler OD 110 mm
PA transducer	Probe with a linear network Nominal frequency 10 MHz Number of elements 16 Inter-element pitch 0,31 mm Elevation 5 mm	Probe with a linear network Nominal frequency 5 MHz Number of elements 64 Inter- element pitch 1 mm Elevation 7 mm
Coupling agent	Thixotropic gel	Water/Thixotropic gel
Chain displacement encoder	----	12 steps/mm

- 3 assemblies implemented with excessive scraping materialized by four flat areas at a 90° angle with a diametrical depth of ca. 1 mm, created using a hand-held rasp to simulate the facets generated by a hand-held scraper (Fig. 3b).
- 3 assemblies with liquid contamination of the fusion zone prior to welding at the level of one of the coupler sockets (Fig. 3c).

Among these 24 assemblies, 8 were devoted to HAZ measurement.

3 Non-destructive Evaluation of the Assemblies by Means of PAUT

The technology used was Phased-Array Ultrasonic Testing—hereafter referred to as PAUT in this document—in Pulse Echo mode. The ultrasonic speed of longitudinal waves in PE100 was set at 2400 m/s. The technical characteristics of the PAUT equipment is listed in Table 2.

When using PAUT with Sector- and Linear-Scanning, the sensitivity calibration was carried out using side drilled hole Ø1.5 mm in a calibration block molded from PE100 for all the focal laws (see Fig. 4). The objective is to attune the detection sensitivity using individual gain correction for each of the focal laws to bring the amplitude of the echoes emitted by the Side Drill Hole (SDH) to 80% of the screen. The gain obtained following this calibration procedure is termed the reference gain, G_{ref} The control gain G_c is defined as the reference gain G_{ref} to which a searching gain of between + 6 dB and + 12 dB is added in order to compensate for the amplitude variations caused by surface conditions, by the small dimensions of the defects sought and by certain defect positions (located close to the electrical connection pins, the fusion indicators or the tapping saddle chimney).

Fig. 1 Distribution of the strips in the so-called mass and crossing configuration

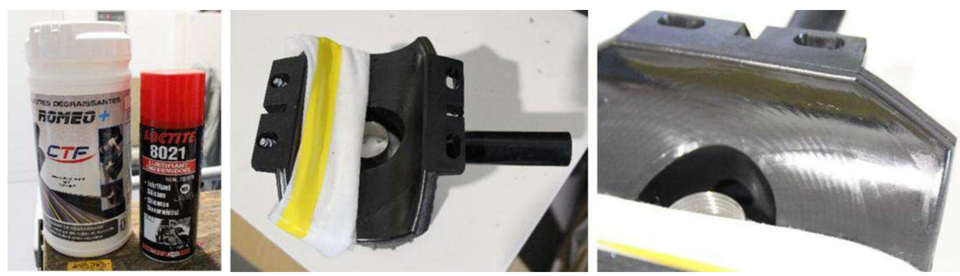

Fig. 2 Liquid contamination by applying spray on one half of the heating zone of the tapping saddle

When using the Total Focusing Method (TFM) in certain cases, the sensitivity calibration was performed directly on the fitting and the gain was adjusted on the wires.

The PAUT control was performed during both the welding phase—at a fixed position of the probe on the tapping saddle and on the coupler—and after complete cooling of the welded assembly, across the complete surface of the welded zone. In the case of control after cooling, the examination was performed, according to two different procedures for pipe-saddles and pipe-couplers assemblies. When examining pipe/saddles assemblies, control is performed manually, without encoding, from the outer wall of the saddle and over every accessible surface of it, as illustrated in Fig. 5. In this case detection relies on longitudinal-wave sector-scanning between − 30° and + 30° by steps of 1° along a radial plane relative to the saddle outlet (0° skew). This type of scan allows ultrasonic beams to be generated under several angles of incidence for a given position of the phased-array transducer. To note for certain defect positions, when standard scanning (0° skew) does not allow the defect to be detected, complementary scanning was performed following a 90° rotation of the probe (90°skew). The ultrasonic waves are then emitted along a tangential plane relative to the saddle outlet.

When examining pipe coupler assemblies, control was performed manually, without encoding, from the outer wall of the coupler and over every accessible surface on it, as illustrated in Fig. 5. In this case, detection relies on longitudinal-wave linear-scanning at 0°. This type of scanning was obtained by electronically moving along a line the active apertures of an array of transducers, without physically moving the phased-array transducer on the assembly. In addition, using Total Focusing Method (TFM) in LL mode (direct mode), mapping was generated by a string-type encoding system.

4 Results and Discussion

4.1 PAUT Control of the Pipe/Saddle- and Pipe/Coupler Assemblies During the Welding Phase

No anomaly was detected during the welding phase of pristine tapping saddles, as evidenced by visual inspection and by electrical parameter measurements (Electrical voltage and intensity). For the nominal heating time, the value of the

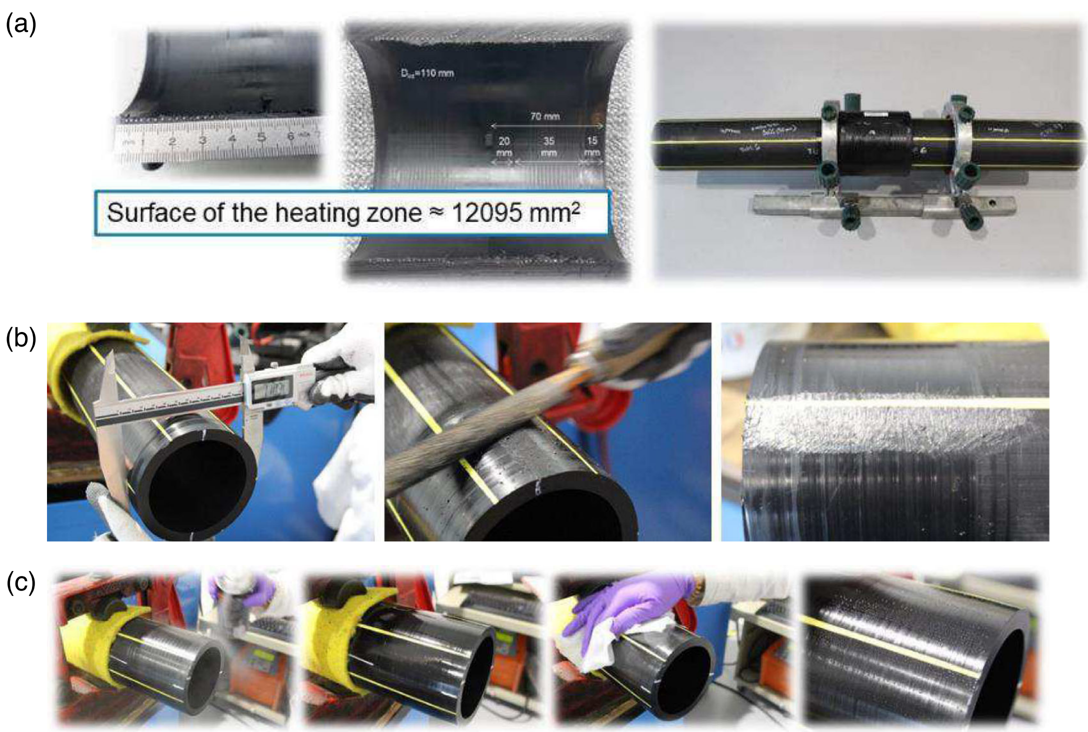

Fig. 3 **a** Incomplete insertion of the DN110 pipe in one of the sleeve sockets. **b** Creating 4 facets at 90° angles using a hand-held rasp. **c** Carrying out a contamination by smearing on one end of a DN110 pipe to be inserted in the coupler socket

Fig. 4 Calibration block (PE100) for PAUT measurements

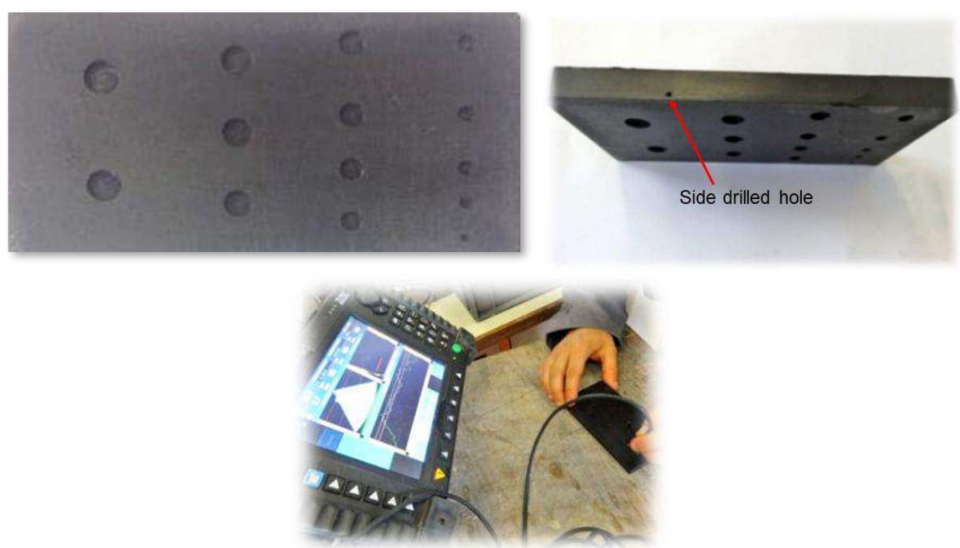

energy delivered by the tapping saddle is very close to the one indicated in the manufacturer's technical documentation.

PAUT control was performed at one fixed point by recording the signals using a time-based encoding (the scanning step is expressed in mm, 1 mm corresponding to 0.1 s). At the measurement point, no significant variation was recorded between the different assemblies. The ultrasonic signals evolve according to the following phases, as illustrated in Fig. 6.

At initial time ($t = 0$): the signals observed are characteristic of those of a non-melted material, with a visualization of the echoes generated by the wires and the saddle bottom wall. For a heating time of ca. 30 s, a gradual increase (dilatation) of the depth of the characteristic initial signal is observed, the progressive heating of the material causing a decrease in the propagation speed. Simultaneously with these variations, a gradual decrease of the saddle bottom wall echo takes place, after approximately 20 s). For a heating time between 30 s and

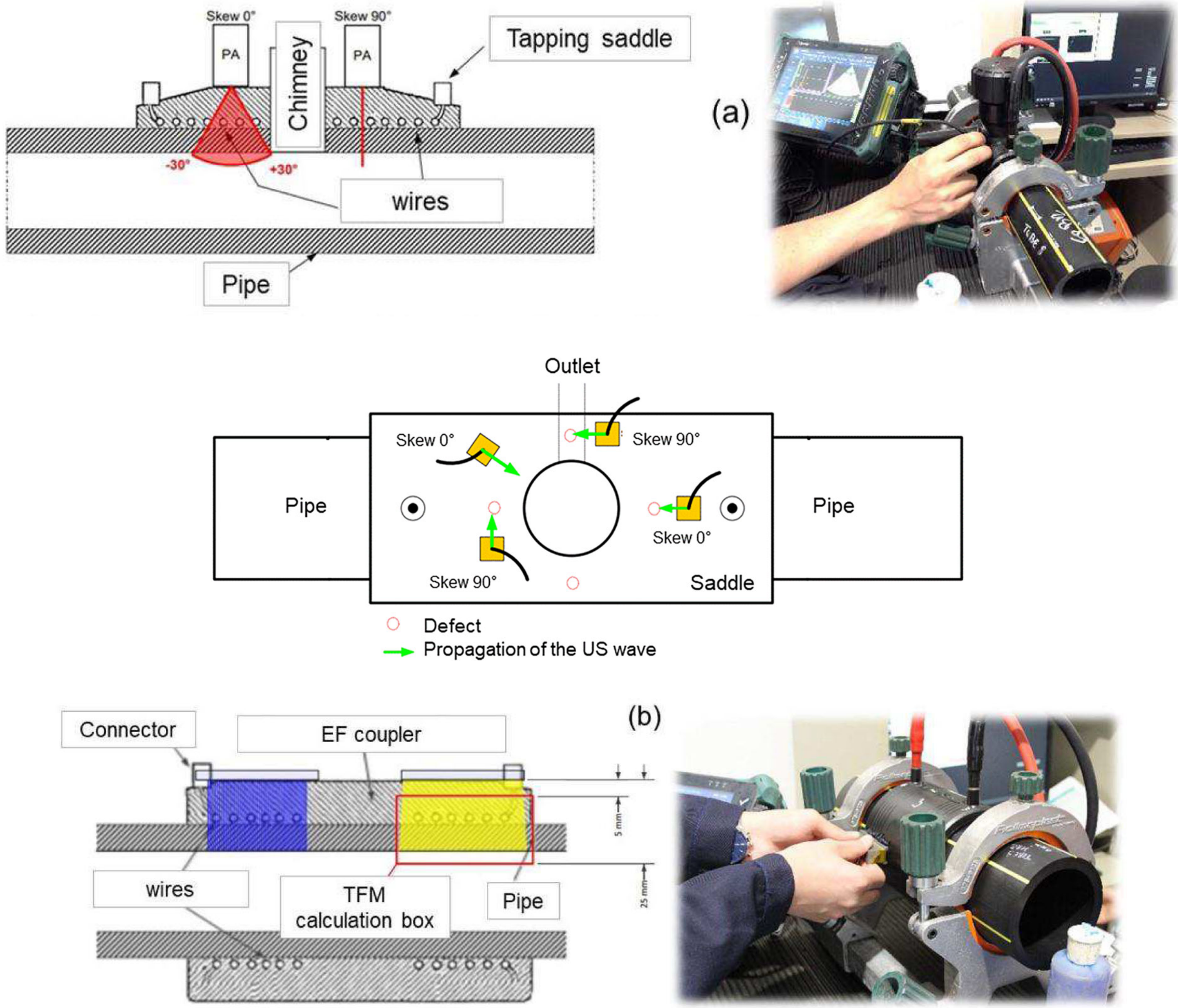

Fig. 5 PAUT control performed on a pipe_saddle (**a**) and pipe_coupler (**b**) assembly during welding

the nominal heating value, an echo appears which probably marks the delimitation between the liquid phase (surrounding the wires) and the solid phase (above and below the wires); during this phase, the distance between this front and the wire position increases. At ca. 42 s the pipe bottom wall echo appears, marking the onset of fusion between the material of the pipe and that of the saddle. The complete disappearance of the interface between the pipe and the saddle is observed at ca. 44 s. Upon reaching nominal time, the onset of cooling is marked by the stabilization of the depth position of the various echoes (wires, pipe bottom wall, upper and lower fusion front). For times exceeding the nominal heating time, the cooling phase leads to a decrease in the depth position of the various echoes and to the gradual disappearance of the echoes marking the limit of the fusion front.

NB: The time lag between the end of heating and the onset of cooling varies between 5 and 15 s, depending on the heating time applied.

The evolution of the various echoes can also be illustrated by C-Scan mapping where the x-axis corresponds to the time from the start of heating (scale expressed in mm, with 10 mm = 1 s) and the Y-axis correspond to the beam angle (from − 30 to 30°), as illustrated in Fig. 7.

4.2 PAUT Control of the Pipe_Saddle- and Pipe_Coupler Assemblies After Cooling

4.2.1 Assessment of the Heat Affected Zone (HAZ) in the Assemblies

Once the assemblies have cooled down, the depth and height of the HAZ are measured for each assembly as displayed in Fig. 8.

NB: Detection of the HAZ boundary is only feasible on the outer of the fitting. Detection of the HAZ on the pipe side cannot be achieved due to the presence of the wire echo.

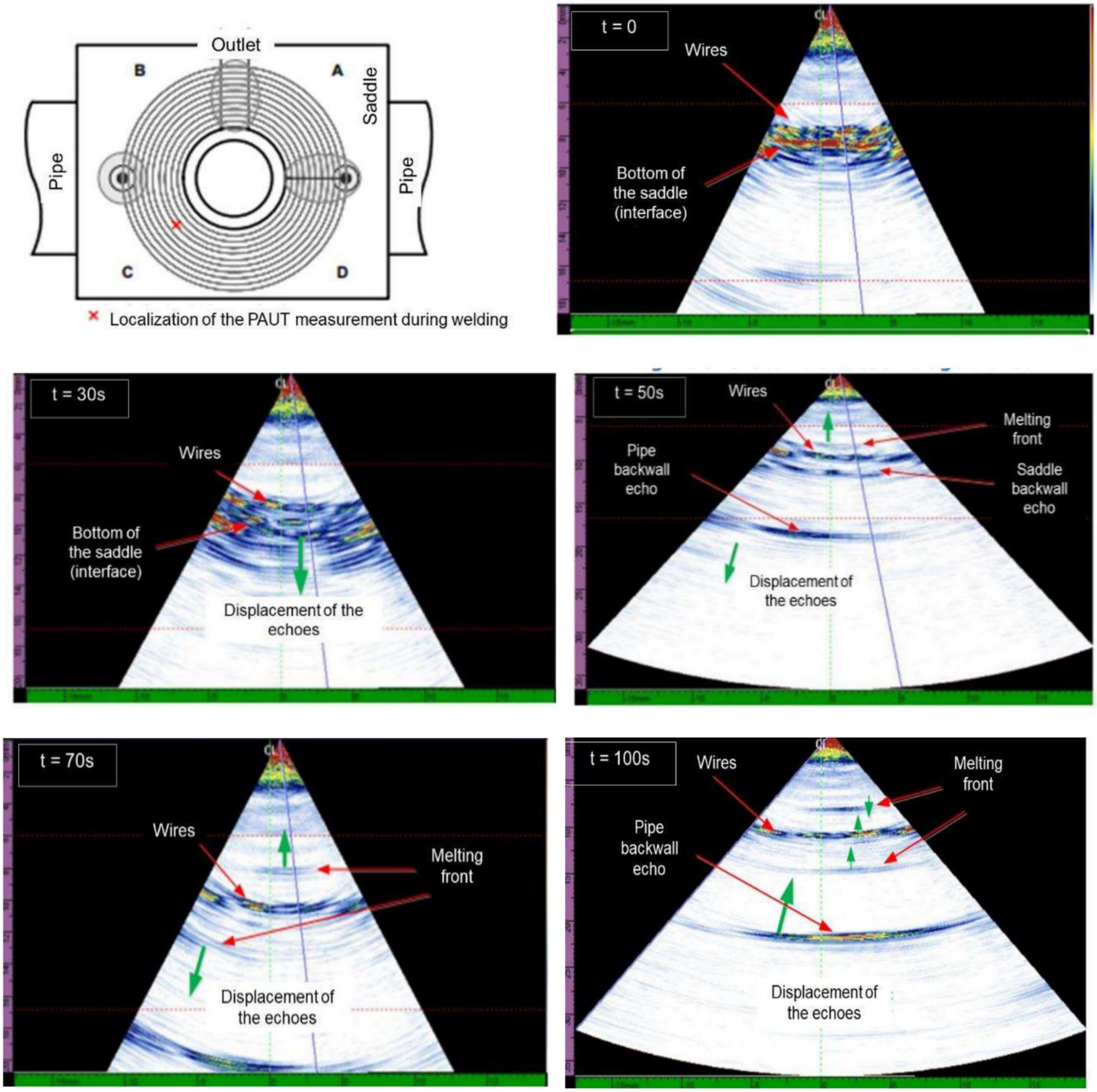

Fig. 6 Position of the PAUT measurement point S-Scans obtained during the monitoring of the welding of saddle assemblies. (NB: in this representation, the saddle is viewed from above, with the fusion indicator to the right representing an area non-accessible to PAUT examination)

The evolution of the HAZ as a function of heating time for the pristine pipe_saddle and pipe_coupler assemblies is displayed in Fig. 9a, b.

For the pipe saddle assemblies, the PAUT measurements scale linearly with heating times. They range between a 0.55 mm average and a 1.7 mm average for heating times corresponding to 55% and 120% of the nominal heating time, respectively. These values represent approximately 1 and 3.5 times the diameter of the saddle wire.

NB: PAUT assessment of the HAZ is based on the mean plane of the heating wires, which exhibit an average diameter of 0.4 mm in the 63 × 20 mm saddles studied here. Furthermore, the wires are embedded within a PE layer whose thickness may be estimated at 0.3 mm, based on observations made using an optical microscope. Therefore, the true values of the HAZ, assessed on the saddle side, must be raised by between 0.3 and 0.4 mm.

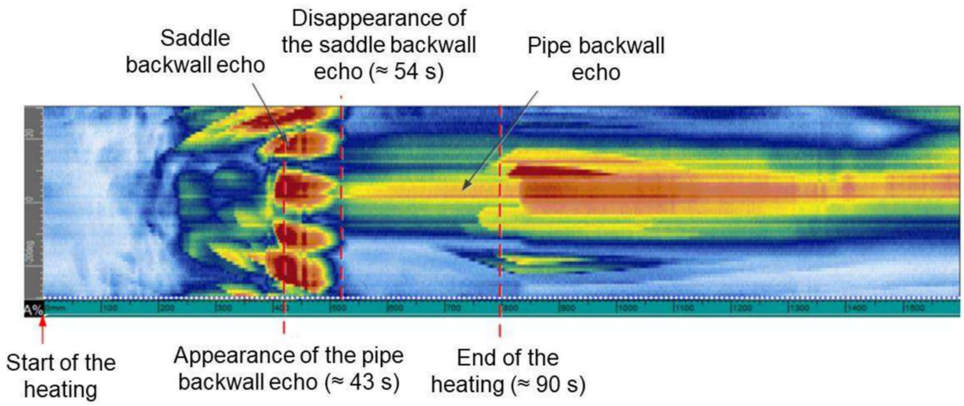

Fig. 7 Time-based C-Scan mapping—Visualization of the evolution of the characteristic signals. NB: The use of a data collection gate means that only signals pertaining to echoes generated by the saddle bottom wall (8 mm thick) and pipe bottom wall (6 mm thick) are displayed in the figure

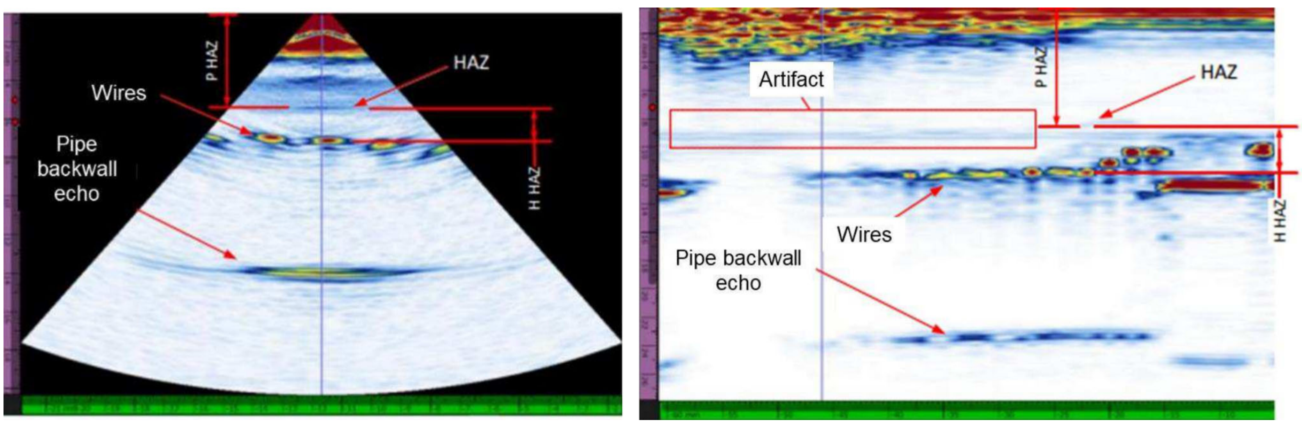

Fig. 8 Measurement principle (S-Scan display) of the Heat Affected Zone for the different assemblies after cooling (Left: saddle; Right: coupler)

In the case of electro welded couplers, it should be noted that a parasitic echo (artefact) is present at a depth close to that of the echo characterizing the outer boundary of the HAZ. This echo interferes with the HAZ measurements on this type of assembly. In addition, the detection of the signal characterizing the HAZ is improved when using a 10 MHz—rather than a 5 MHz frequency. Since the couplers must be controlled using a 5 MHz probe to restrict signal attenuation, detection of the HAZ echo is therefore impaired compared to the saddle measurements for which a 10 MHz probe is used.

PAUT measurements show that the HAZ height varies from an average of 1.4 mm to an average of 3.5 mm for heating times corresponding to 55% and 120% of the nominal heating time, respectively. These values represent approximately 2.5 and 6 times the diameter of the sleeve wire. For welding implemented at nominal heating time, the HAZ height ranges between 2.9 and 3.0 mm.

NB: PAUT assessment of the HAZ is based on the mean plane of the heating wires, which exhibit an average diameter of 0.6 mm in the DN110 coupling sleeves studied here. Furthermore, the wires are embedded within a PE layer, whose thickness does not feature in the manufacturer's technical documentation. It may nonetheless be estimated at 0.5 mm based on observations made using an optical microscope. Therefore, the true values of the HAZ, assessed on the saddle side, correspond to the relative values presented here but raised by a value of ca. 0.8 mm.

Figure 10a, b displays the HAZ values obtained for all the pipe_saddle- and the pipe_coupler assemblies welded at the nominal heating time

For the pipe saddle assemblies, the HAZ height varies between 1.15 mm (B12) and 1.55 mm (C11, C12) for the nominal heating time. On average, the HAZ values are ca. 1.33 mm for assemblies featuring strips in "mass" configuration, ca. 1.39 mm for assemblies featuring strips in "crossing" configuration and ca. 1.30 mm for assemblies subjected to liquid contamination, compared to the average of ca. 1.38 mm obtained for assemblies devoid of induced defects. These averages are similar and, therefore, the PAUT-assessed HAZ height on the saddle side may be deemed to be unaffected by the presence of defects implanted at the pipe/saddle interface.

For the pipe coupler assemblies, except for the assembly implemented with an overly insufficient socket insertion, corresponding to 50–60% of the heated zone instead of the recommended 80%, and which had to be deliberately interrupted at 68% of the nominal heating time following smoke emission, the HAZ values are ca. 2.8 mm on average for

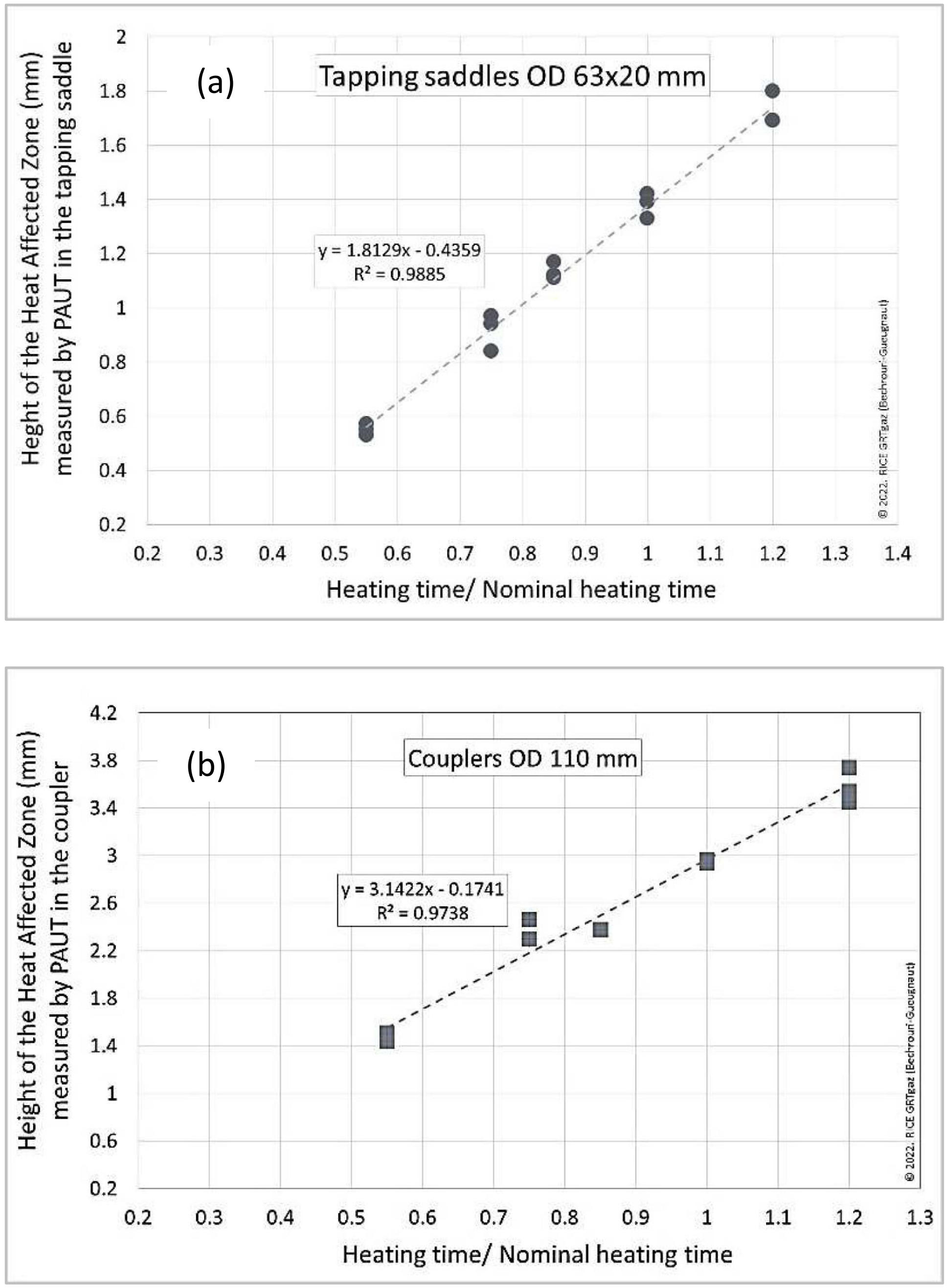

Fig. 9 Height of the HAZ after cooling as a function of heating time in the pristine pipe_saddle (**a**)- and the pipe_coupler (**b**)- assemblies

assemblies implemented with incomplete socket insertion, ca. 3.0 mm on average for assemblies exhibiting excess scraping (4 facets at 90° angle) and ca. 2.9 mm on average for assemblies subjected to liquid contamination, compared to the 2.9 mm average obtained on assemblies devoid of induced defects. Within measurement uncertainty, all these values are similar and, consequently, the HAZ height on the sleeve side is not affected by the presence of the faults at the pipe_coupler interface.

4.3 Detection and Sizing of the Faults in the Different Assemblies

The saddles were controlled by manual moving of the probe while applying a sector-scan. Mapping of the defect zones was subsequently performed based on the recorded data. Figure 11 shows, as an example, a mapping of the unwelded zones for three different heating times.

The PAUT controls reveal the presence of unmelted areas in assemblages carried out by applying a heating time corresponding to 55% and 75% of the nominal heating time.

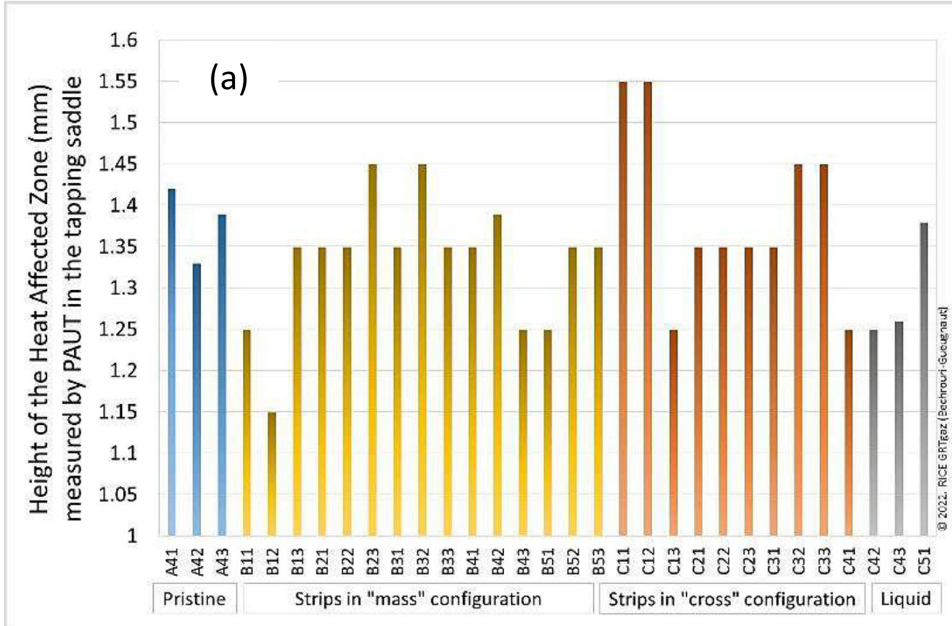

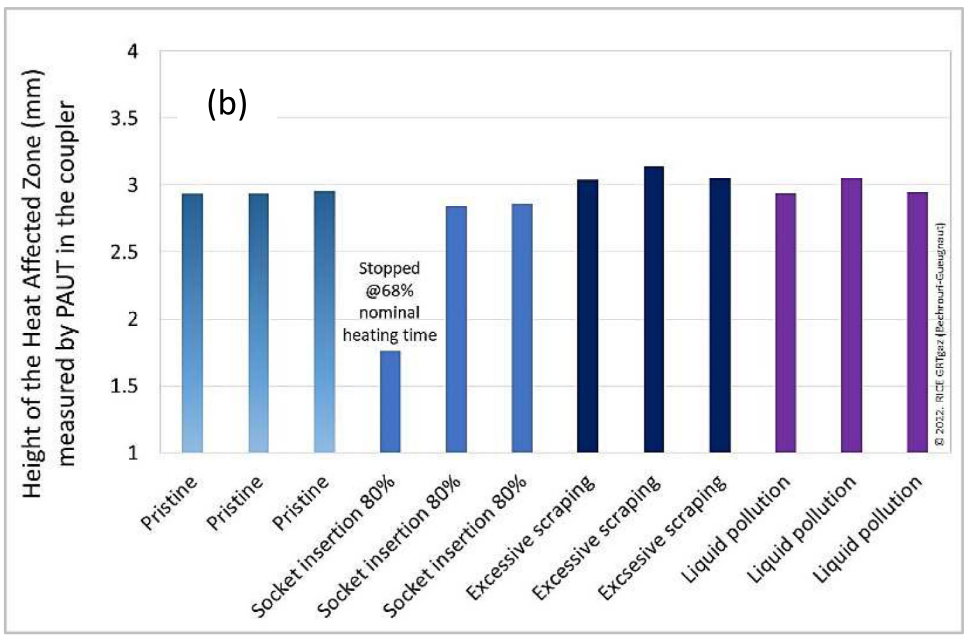

Fig. 10 HAZ height after cooling for the pipe_saddle- (**a**) and the pipe_coupler- (**b**) assemblies. HAZ is measured respectively on the saddle side and on the coupler side

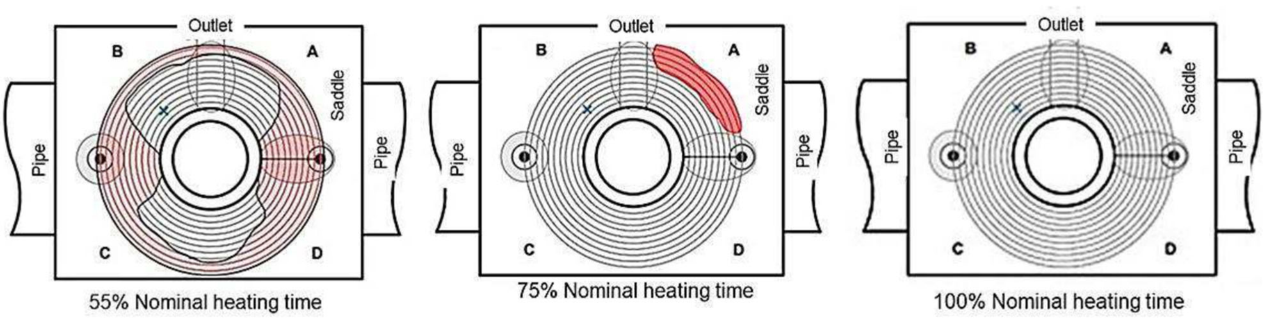

Fig. 11 PAUT schematic maps of the pipe_saddle assemblies at heating times of 55%, 75% and 100% of the nominal heating time (in red: unmelted area) (Color figure online)

These unmelted zones are located mainly at the outer edge of the heating area and in the vicinity of the wire connectors. As expected, fusion starts in the central part of the heating zone—where the temperature increase is fastest due to the high concentration of adjacent wire coils—and then spreads gradually towards the outer edge. For a heating time corresponding to 55% of the nominal time, unmelted zones account for nearly 50% of the total surface. For heating times equal to or longer than 85% of the nominal value, no fusion defects were revealed by the PAUT controls.

Figure 12 shows, as an example, the mapping of the saddles with strips in "mass" configuration implanted on the heating area, welded at the nominal heating time.

PAUT controls result in the detection of 94.4% of the reflectors implanted in mass configuration prior to welding. The remaining undetected 5.6% correspond to reflectors positioned at locations for which measurement is difficult (close to the connectors or to the saddle chimney).

The sizing of indications is performed manually by moving the probe around the indication zone and applying a − 6 dB sizing, as illustrated in Fig. 13. Given the complex geometry of the assembly (curvature + striations on the outer wall), this measurement remains an approximation. Furthermore, in some cases the end of the indications cannot be detected due to the presence of geometrical obstacles (in the vicinity of the saddle chimney, the branching outlet or the fusion connectors), which means that the values are probably underestimated.

Figure 14a, b displays PAUT measurements of unwelded areas (H: width and L: length) in relation to the actual size of the reflectors implanted in "mass" configuration on the heating layer of the tapping saddles

Sizing of the unwelded zones is possible in more than 95% of the configurations:

- with a length equal to or longer—even far longer—than the true length of the implanted strips in 100% of cases, regardless of the amount of the inserted reflectors.
- with a width larger than the true width of the implanted strips in ca. 52% of cases; the small value of the strips' actual width, together with access difficulties for the ultrasonic transducer in the vicinity of the connectors and the saddle chimney, hinder measurement, resulting in the underestimation of the width of the strips in 48% of cases.

For the assemblies with strips in "crossing" configuration, about 95% of the reflectors are detected at the interface. The remaining, undetected 5% correspond to reflectors positioned at locations for which measurement is difficult (close to the connectors or to the saddle chimney). Sizing is possible in 84% of the cases:

- with a length equal to or longer—even far longer—than the true length of the implanted strips in 55.5% of cases, this up to a length corresponding to 40% of the width of the heating zone. At the threshold value of 50% of the width of the heating zone, the PAUT measurement underestimates the length of the unwelded zone by ca. 9%. For a length corresponding to 63.6% of the heating zone, the PAUT measurement underestimates the length of the unwelded zone by ca. 29%.
- with a width larger than the true width of the implanted strips in ca. 81% of the measurable cases; the small value of the strips' actual width, together with access difficulties for the ultrasonic transducer in the vicinity of the electrical connectors and of the saddle chimney, hinder measurement, resulting, in 19% of cases, in the underestimation of the width of the strips.

PAUT and TFM controls of the pipe_coupler assemblies with incomplete pipe insertion in one of the sockets is presented in Fig. 15. For comparison purposes, one of the assemblies was also examined using X-ray radiography.

The improper pipe insertion is clearly revealed by the three techniques but with quite different resolutions. It translates as a pipe bottom echo with a reduced width. The melted zone is estimated to about 15 mm (instead of 35 mm). For the other two assemblies, in view of the difficulties that arose during welding, the length of improper insertion was shortened. It resulted in the anomaly being more difficult to detect in this case. Several hypotheses may be put forward to explain this: the portion of the fusion zone with no contact between the pipe and the sleeve is very close to the edge of the fusion zone itself (variation of the pipe bottom echo estimated at 3 mm, compared to the standard case), leading to a confusion between the unmelted zone and the edge beside of the central part of the sleeve. When fusion occurs, the part of the sleeve that does not overlay the pipe becomes distorted and creates a non-parallel geometry relative to the control surface, which translates as a poor reflection of the ultrasonic waves. Therefore, detection of this type of defect becomes a function of the length of the improperly inserted part of the pipe. Depending on the size characteristics of the sleeves (distance to the central stopper, width of the fusion zone provided by the manufacturer, position of the heating coil in the assemblage) a theoretical minimum value for detection could be given.

Figure 16 displays an example of the results of standard- and TFM PAUT controls performed on assemblies implemented with excessive scraping of the pipe, materialized by four facets at 90°.

PAUT and TFM controls reveal the presence of zones exhibiting improper fusion which coincide with the facets created by excessive scraping. The unmelted zones are localized at the outer and the center edges of the fusion zone and

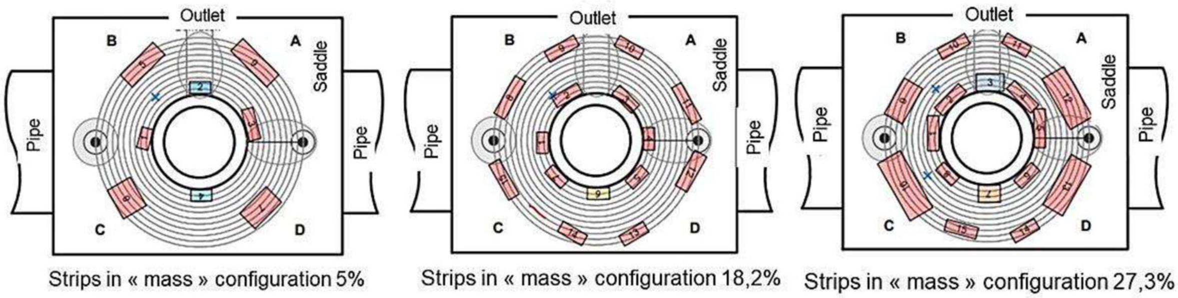

Fig. 12 Maps of the assemblies featuring strip-like defects distributed in "mass" configuration on the heating layer of the sleeve (welded at nominal heating time) (in red: defect area) (Color figure online)

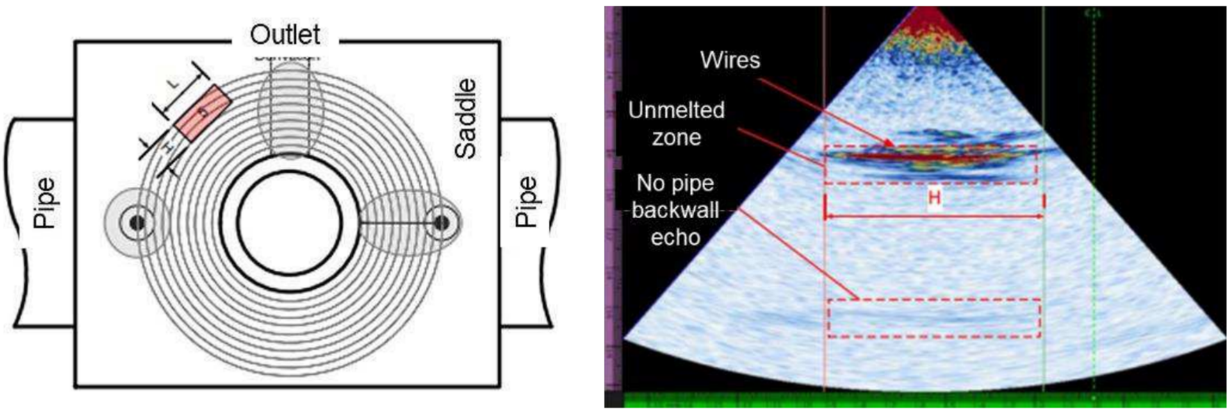

Fig. 13 Sizing of defects in pipe_saddle assemblies welded at nominal heating time

thus are not visible in their central part. The length of these zones varies between 3 and 6 mm for a width of ca. 20 mm.

4.3.1 Comparison Between the Real Implanted Defects and Those Detected Using PAUT

A comparison of the surface area of the physically implanted strips with that of the disorders sized using PAUT can be done. The target surfaces represented by the defects (ratio of the total surface of the sum of the strips to the surface of the heating zone, ca. 4400 cm^2) are compared to those measured using PAUT based on the sizing of individual strips. The calculation is made using the theoretical width and height values of the strips and their equivalent estimated by PAUT.

Figure 17a–c displays the PAUT sizing values for the disorders ascribed to defects in "mass" (a)- and "crossing" (b) configuration, against the physical dimensions of the implanted defects

The surfaces occupied by either "mass" or "crossing" defects, as measured by PAUT, are much larger than those occupied by the physically implanted defects. The strips generate disorders in their vicinity by interfering with the heat exchanges. This is verified by further examination of the decohesion surfaces. For a target relative surface of 5% for implanted "mass" defects, the value measured by PAUT is almost double this figure, while for a target surface of 27.3%, the value determined by PAUT is approximately 37%.

Except for one case—characterized by an insufficient dataset—the surface occupied by "crossing" defects as measured by PAUT is much larger than that occupied by the physically implanted strips. Moreover, the length of the "crossing" defects, as measured by PAUT, exceeds that of the implanted strips up to 40% of the width of the saddle heating layer. Beyond this value, PAUT underestimates the true value of the physically implanted defect, with assessed values of the order of 45% of the width of heating layer. Such underestimation can be attributed to the difficulties to access some zones of the saddles with the ultrasonic transducer.

4.4 Destructive Testing of the Saddles and Couplers After Cooling

4.4.1 Sizing of HAZ

To measure the HAZ in the tapping saddle assemblies, these are cut in 8 pieces and the HAZ is revealed by heating the material along the cuts at a 90° angle to the interface using a heat-gun. The heat treatment reveals the differences

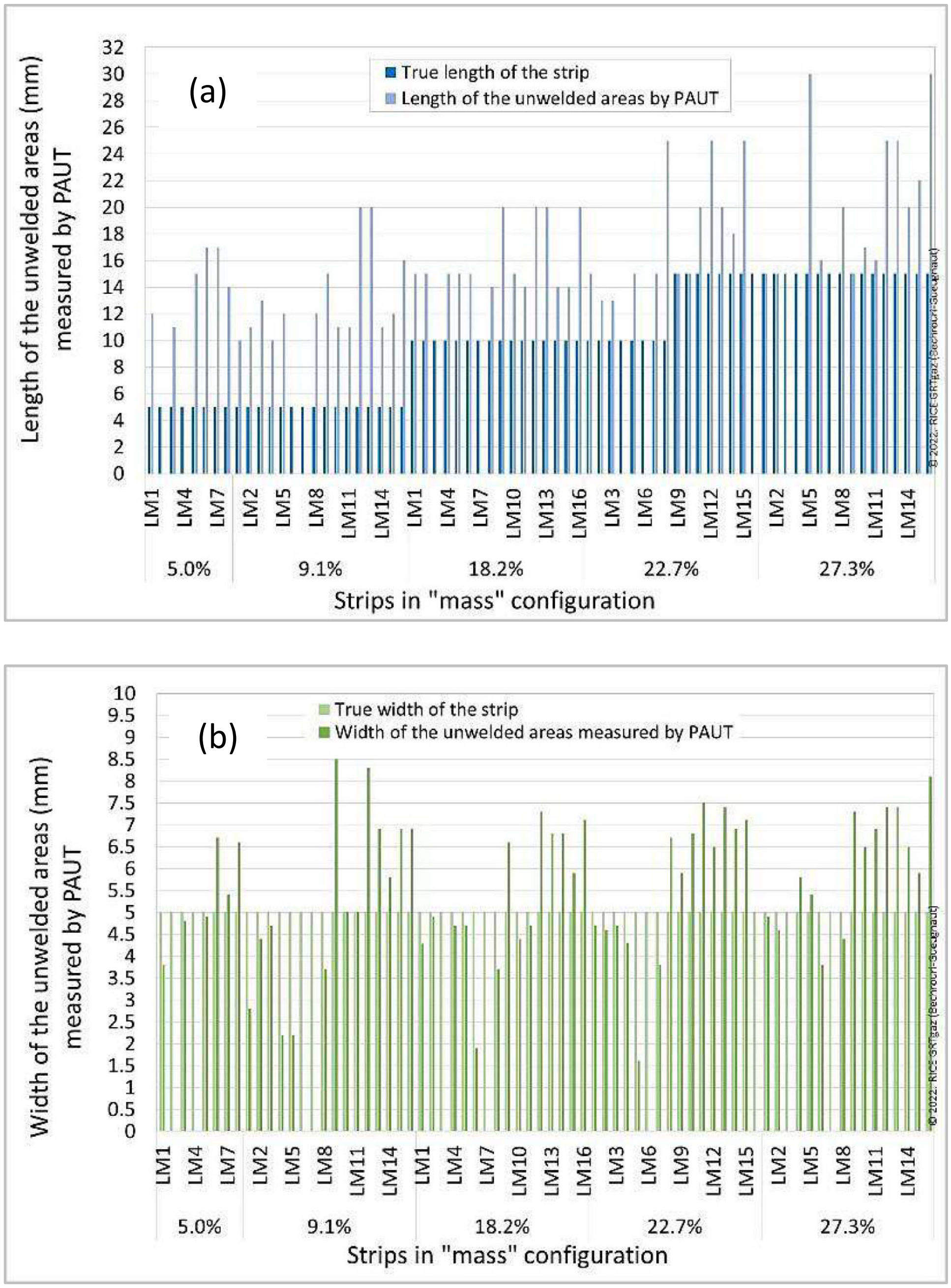

Fig. 14 Comparison of PAUT measurements of unwelded zones with the true dimensions of the strips in mass configuration implanted on the heating plane of the tapping tee prior to welding (**a** length; **b** width)

in crystalline structure generated by the differential heating and cooling of the material surrounding the interface during welding [38]. HAZ measurement is then performed using an optical stereo microscope equipped with a measuring reticle accurate to 1/100 of a millimeter. The same treatment is applied on the pipe_coupler assemblies, cutting them in six strips (see Fig. 18).

The graphs in Fig. 19a–c display the correlation between the HAZ measurements obtained using PAUT on the saddle- and the coupler side and the corresponding values of the total height (pipe side + fitting side) obtained by direct examination of the cross-sections.

There is a fair correlation between the non-destructive method and the measurement-after-cutting approach. The most probable linear regression curves for this dataset show that the 'blind' assessment makes it possible to predict the total height of the HAZ from the height assessed by PAUT with a slight overestimation of the true value measured after cutting.

Thus, for the saddles welded at the nominal heating time, the total height of the HAZ may be estimated at ca. 3.6 mm

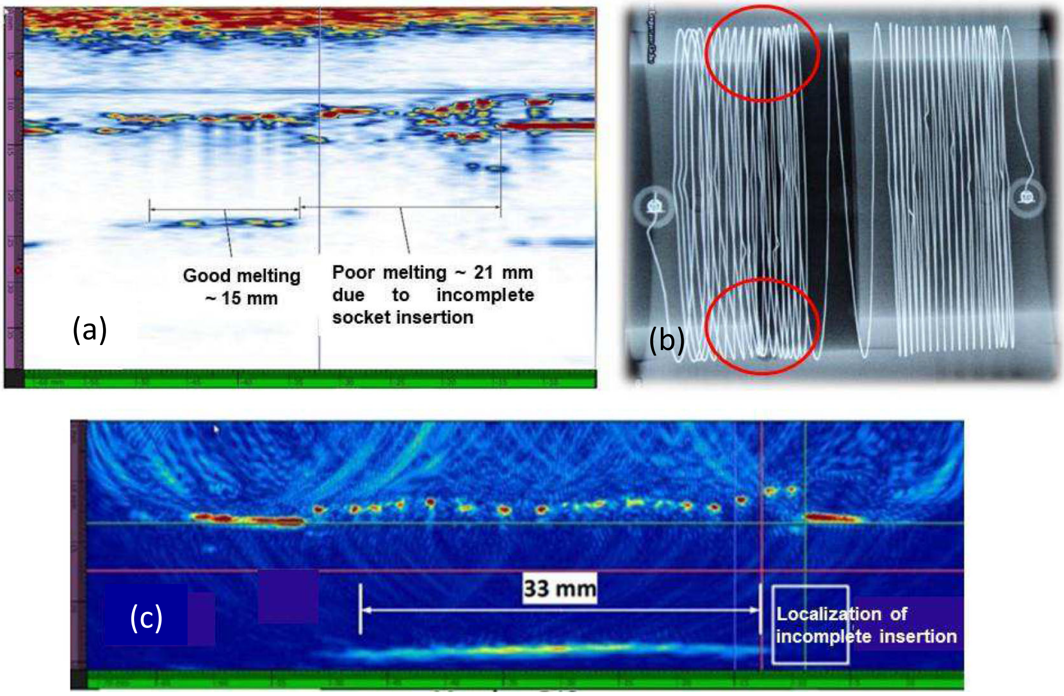

Fig. 15 Examples of B-Scan, X-Ray and TFM displays of assemblies implemented with incomplete pipe insertion in one of the coupler sockets. **a** PAUT B-scan of large incomplete socket insertion; **b** X-ray image of incomplete socket insertion; **c** TFM image of small incomplete socket insertion

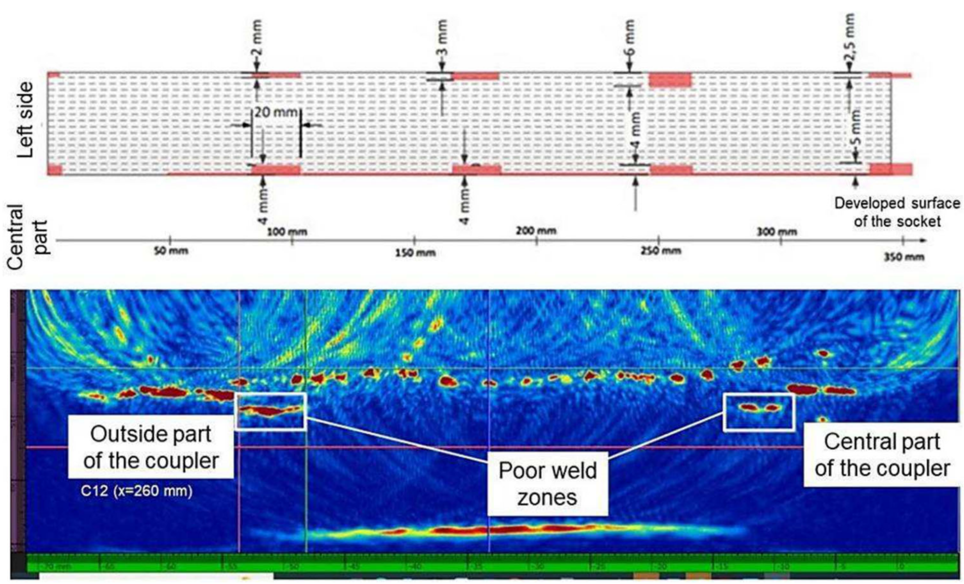

Fig. 16 Examples of standard PAUT and TFM display for assemblies implemented with excessive scraping of the pipe (4 facets at 90° angle) inserted in one of the coupler sockets

to 3.8 mm, for a height on the saddle side of 1.4 mm above the mean plane of the wires.

Taking into account what has been explained above, for the true value of the HAZ on the saddle side to be obtained, one needs to add, on the one hand, half the wire diameter (ca. 0.2 mm), and, on the other hand, the thickness of the PE layer embedding the wires in contact with the pipe (ca. 0.3 mm) to the 1.4 mm value, hence a total value of 1.9 mm in the saddle (from the pipe interface) and of 1.7 mm to 1.9 mm on the pipe side.

For the couplers welded at the nominal heating time, the total measured height of the HAZ is ca.5.5 mm, for a PAUT estimated height on the sleeve side of ca.2.9 mm above the mean plane of the wires. As for the saddle, the true value

Fig. 17 PAUT estimates of the surfaces occupied by the defects in “mass” configuration (**a**) and of the lengths occupied by the defects in “crossing” configuration (**b**, **c**)

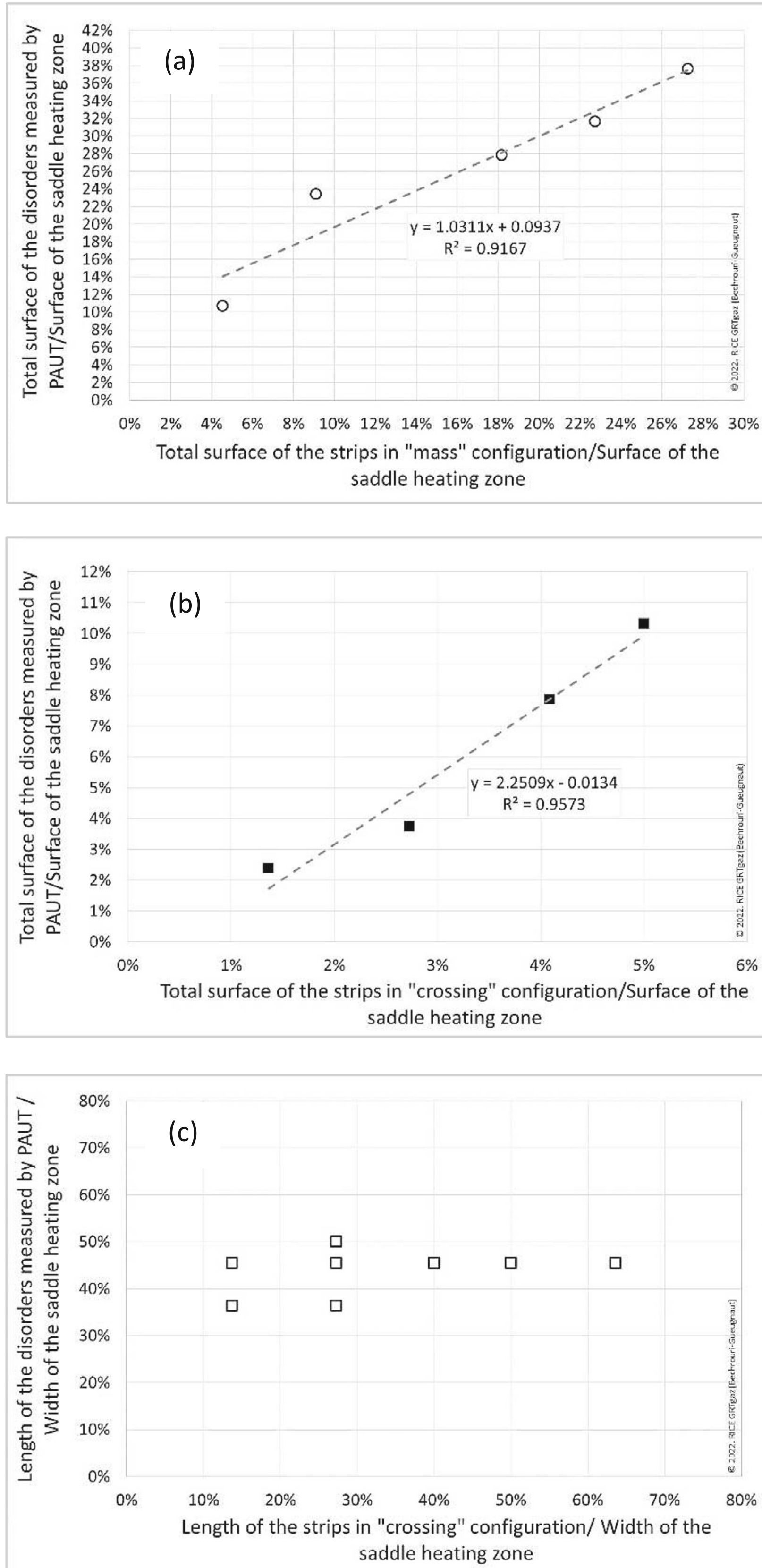

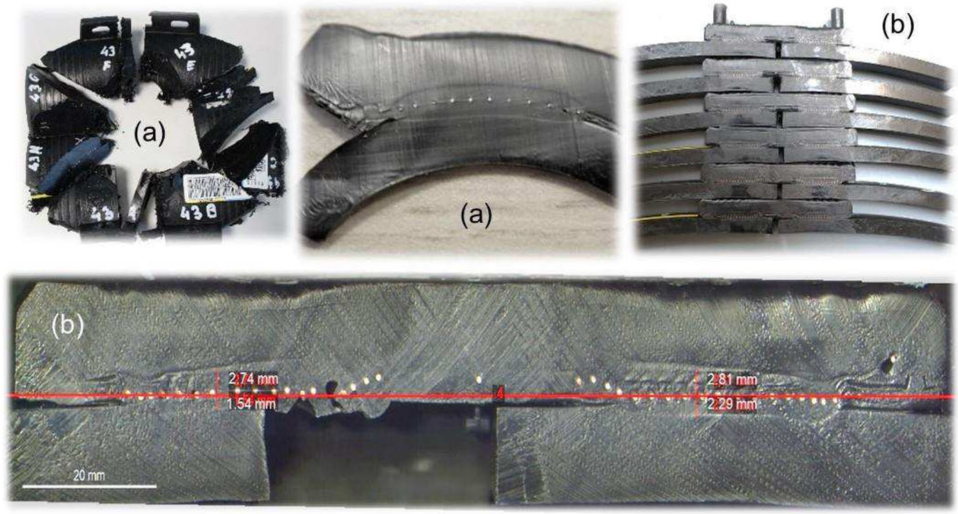

Fig. 18 HAZ measured on cross-sections taken from both pipe_saddle- (**a**) and pipe_coupler assemblies with incomplete insertion of the pipe in one of the sockets of the coupler (**b**)

of the HAZ on the coupler side is obtained by adding, on the one hand, half the wire diameter (i.e. 0.3 mm) and, on the other hand, the thickness of the PE layer embedding the wires in contact with the pipe (ca. 0.4 mm) to the 2.9 mm value, hence a total value of 3.6 mm in the coupler (from the pipe interface) and of ca.1.9 mm on the pipe side instead of ca.3.1 mm by direct measurement on the cross-sections. The poor correspondence between these results is due mainly to the scattering of the measurements on the cross-sections of the pipe_coupler assemblies. It is worth noting that at the nominal heating time, the values are quite similar for the pristine coupler and those with either liquid pollution or excessive scraping. At the contrary, the coupler with the incomplete insertion—even welded at the nominal heating time—has far lower values, which are very close to those of the couplers welded at between 55 and 75% of the nominal heating time. These lower values at both sides suggest that the incomplete insertion in one of the sockets has an influence in the other socket.

4.4.2 Hydrostatic Pressure Testing of the Different Assemblies

The resistance of the welded assemblies was tested according to the conditions recommended by the NF EN 1555-3 standard, namely, at a temperature of 80 °C for a hoop stress of 5 MPa. Under these conditions, the minimum failure time required is 1000 h. The pipes were pierced using the integrated perforator of the saddle, after a 24 h-minimum cooling time (see Fig. 20).

Figure 21 displays the results of the hydrostatic pressure test on pipe_saddle assemblies with defects, welded at the nominal heating time.

The data show that all the assemblies with defects comply with the minimum requirements of the ISO standard. Based on this test, no clear trend emerges regarding the impact on the failure time of both the proportion and the type of the implanted defects at the interface.

For the pipe_saddle assemblies, the failure is located either at the level of the welding interface (diffuse leakage) in 37.5% of cases, at the level of the fusion indicator in 31% of cases, or at the level of the body of the saddle in 28% of cases. Considering the type of assembly shows that leakage occurs:

- Predominantly at the interface for the pristine assemblies implemented at varying heating times.
- In virtually equal proportions at the level of the interface, the fusion indicator, and the body of the saddle for assemblies with "mass" strips at the interface; when the strips are inserted in "crossing" configuration, the leak tends to occur preferentially at the level of the fusion indicator and the interface.
- Indifferently at the interface or in the body of the saddle for assemblies with liquid contamination of the interface. This result strongly depends on the reproducibility of the way the liquid contamination is applied prior to welding.

Figure 22 displays the results of the hydrostatic pressure test on pipe_coupler assemblies with defects.

The data show that all the pipe_coupler assemblies with defects comply with the minimum requirements of the NF EN 1555 standard. The failures occur in the body of the coupler, with an initiation site at the border of the most internal wire of the socket where the stress concentration is the highest, as expected [39]. Based on this test, no clear trend emerges regarding the impact of the type of defects at the interface on the failure time.

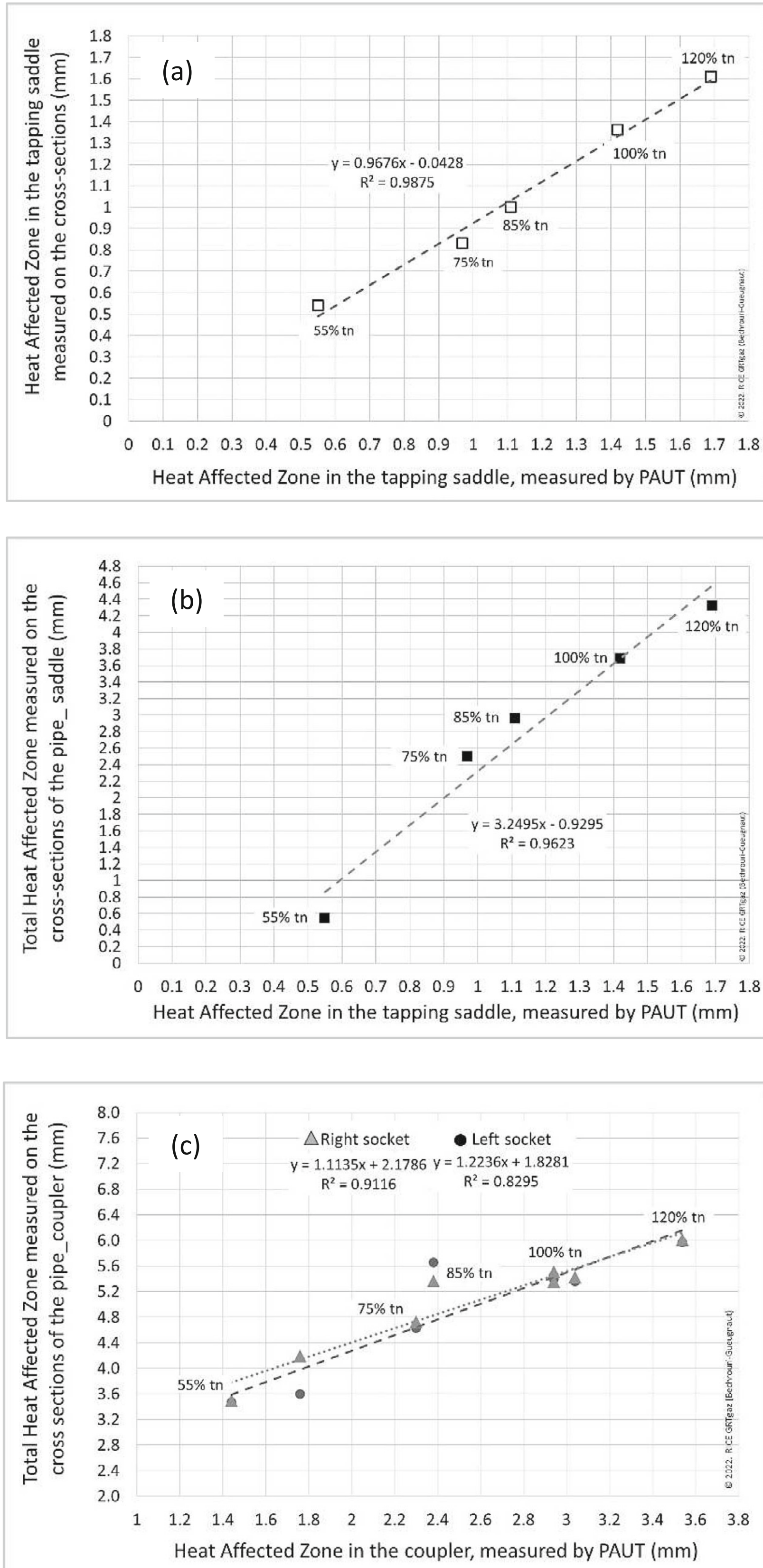

Fig. 19 Comparison of the HAZ heights assessed using PAUT and the measurements performed on the cross-sections for pipe_saddle (**a**, **b**) and pipe_coupler (**c**) assemblies

Fig. 20 Assemblies implemented for the hydrostatic pressure tests

Configuration of the defects at the pipe_saddle interface	Mean failure time / NF 1555 requirement
5.0% Mass	1.67
9.1% Mass	1.79
18.2% Mass	2.09
22.7% Mass	1.90
27.3% Mass	1.39
13.7% Cross	1.61
27.3% Cross	1.10
40.0% Cross	1.91
50.0% Cross	1.33
63.6% Cross	1.52
Liquid pollution	1.46

Fig. 21 Results of the hydrostatic pressure tests performed on the pipe_saddle assemblies with defects at the interface, welded at nominal time. The photo illustrates a leaking assembly resulting of a failure at the interface

Configuration of the defects at the pipe_coupler interface	Failure time / NF 1555 requirement
55% tn	3.0
75% tn	1.2
85% tn	2.0
100% tn	1.8
120% tn	2.4
100 tn_80% socket insertion	2.0
100% tn_excessive scraping	3.0
100% tn_liquid pollution	1.3

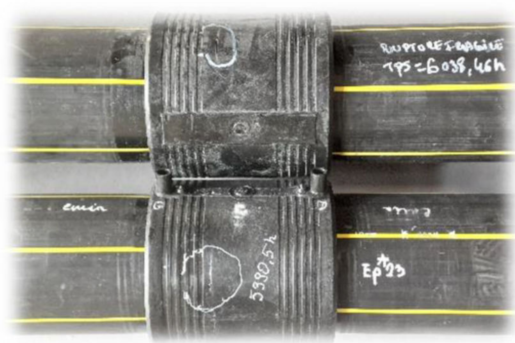

Fig. 22 Results of the hydrostatic pressure tests performed on the pipe_coupler assemblies with defects

4.4.3 Tear Testing After Hydrostatic Pressure Tests

The saddle assemblies that underwent rupture during HPT have been subjected to a peel decohesion test, based on the ISO 13956 standard (A2 Configuration).

Figure 23a–c displays some examples of decohesion surfaces obtained for pristine saddles and for saddles with implanted defects

As expected, at the shortest heating time (55% t_n), the surface is strictly brittle with only a few scattered sticking zones reflecting the lack of fusion of the material. Conversely, at the longest heating time (120% t_n), the fracture surface is strictly ductile and incisions with a craft knife are needed to initiate the entire decoupling of the interface.

For assemblies with "mass" defects in proportions at both ends of the spectrum (P10 and P2), the decohesion surfaces

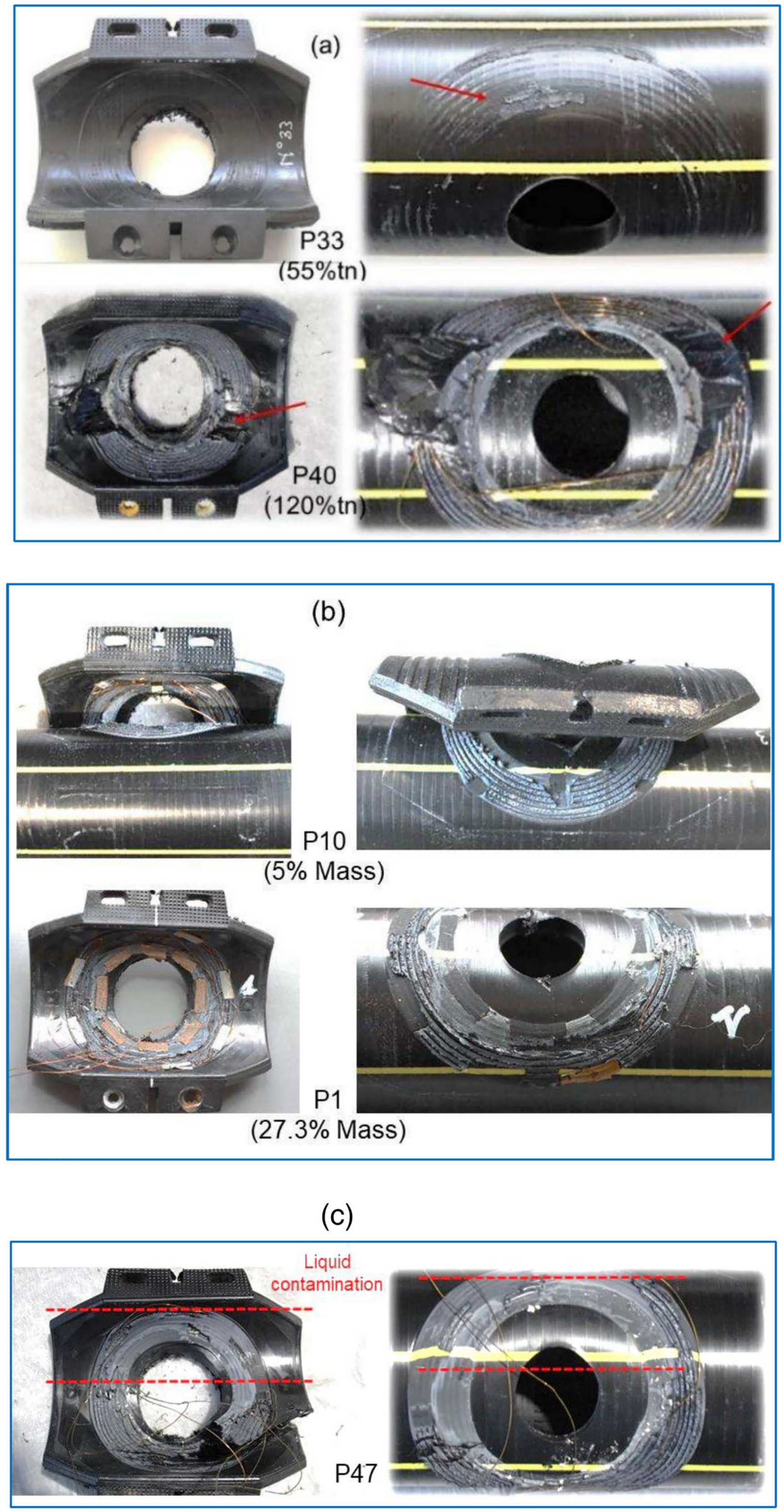

Fig. 23 Decohesion surfaces of pipe_saddle assemblies. **a** Assemblies welded at 55% and 120% of the nominal heating time; **b** Assemblies with 5% and 27.3% “mass” strips; **c** Liquid contamination on one half of the heating zone

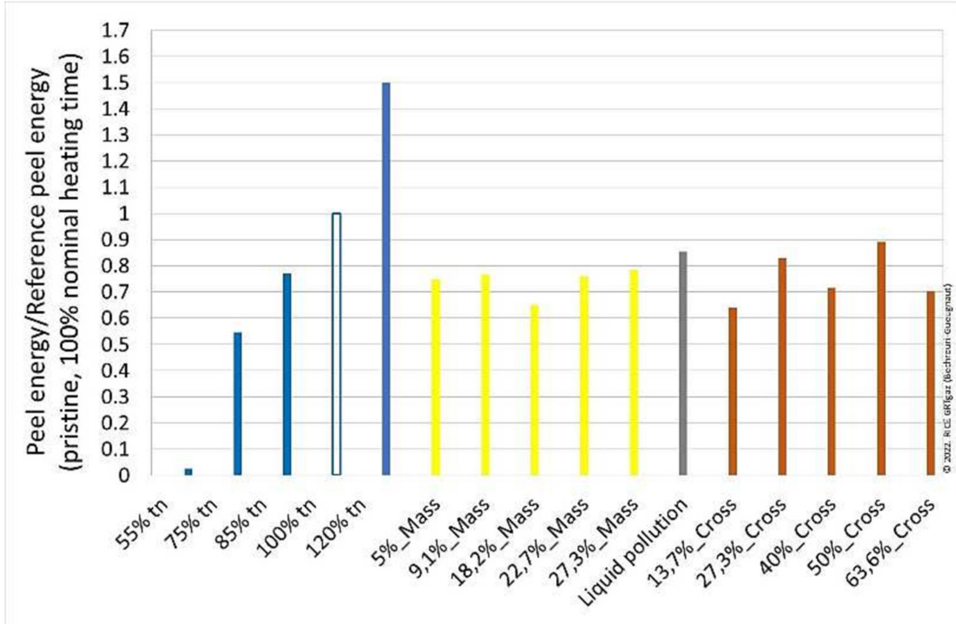

Fig. 24 Normalized peel energy following hydrostatic pressure tests of pristine and faulty pipe_saddle assemblies

are mainly ductile with a few brittle zones weakly spread around the strips.

The liquid contamination of one half of the tapping tee becomes materialized as a brittle fracture surface on the branching outlet side, while the other, non-contaminated half exhibits a ductile surface.

The values of the tear energy obtained by integrating the area beneath the peeling curves for the various assemblies and normalized by that of the reference one (pristine saddles welded at the nominal heating time), are presented in Fig. 24.

The peel energy ratio ranges between less than 0.1 to 1.5 for pristine saddles welded at between 55 and 120% of the nominal heating time. This shows that, despite the thermomechanical history resulting from the hydrostatic pressure test, the hierarchy in terms of decohesion strength is upheld as far as the assembly heating time is concerned. Nevertheless, for the assemblies welded at the nominal time, the average value is 2-to-3 times lower that determined in prior works for pristine tapping saddles of the same model but that did not undergo hydrostatic pressure testing before the peeling test [26, 30]. The lower reference value for the tear test could be a consequence of the HPT solicitation prior to peel testing of the pristine pipe_saddle assemblies.

The peel energy ratio for faulty assemblies is of the order of 0.75 for both "mass" and "crossing" strips and of the order of 0.85 for liquid pollution; These values are very close to that obtained on the pristine saddles welded at 85% of the nominal heating time.

Consequently, a decohesion test performed following hydrostatic pressure testing, even though it allows the impact of the heating time and of the presence of interfacial defects on the peeling energy to be assessed, is not discriminative in terms of both the type and the proportion of defects.

4.4.4 Comparison Between the Disorders Detected Using PAUT and Those Observed on the Peeled Surfaces Following Hydrostatic Pressure Tests

In the absence of any quantitative processing of the optical microscope examination of the decohesion surfaces—like what has been done in a previous study [26, 30]—comparisons with the PAUT measurements only remain qualitative in the frame of this study, given the more than likely disturbance of the prior hydrostatic pressure testing.

Figure 25 presents some examples of confrontation between disorders at the pipe_saddle interface assessed by PAUT and the corresponding decohesion surfaces following hydrostatic pressure testing.

Comparison of the disorders on the pristine assemblies shows that in the case of welding at 55% of the nominal heating time, the PAUT technique detects approximately 50% of weak cohesion zones, while the decohesion surface appears as 100% unwelded. In the case of welding at 85% of the nominal heating time, the PAUT technique does not detect any weak cohesion zone, while the decohesion surface reveals a brittle zone, concentric to the saddle chimney and visually accounting for over 70% of the surface of the heating zone. However, this comparison must be treated with caution in view of the geometry of this brittle zone which might correspond to the water exit pathway during the hydrostatic pressure test.

Fig. 25 Disorders at the pipe_saddle interface assessed using PAUT and those observed on the decohesion surfaces following hydrostatic pressure testing, for pristine assemblies welded at various heating times and assemblies with implanted "mass" defects

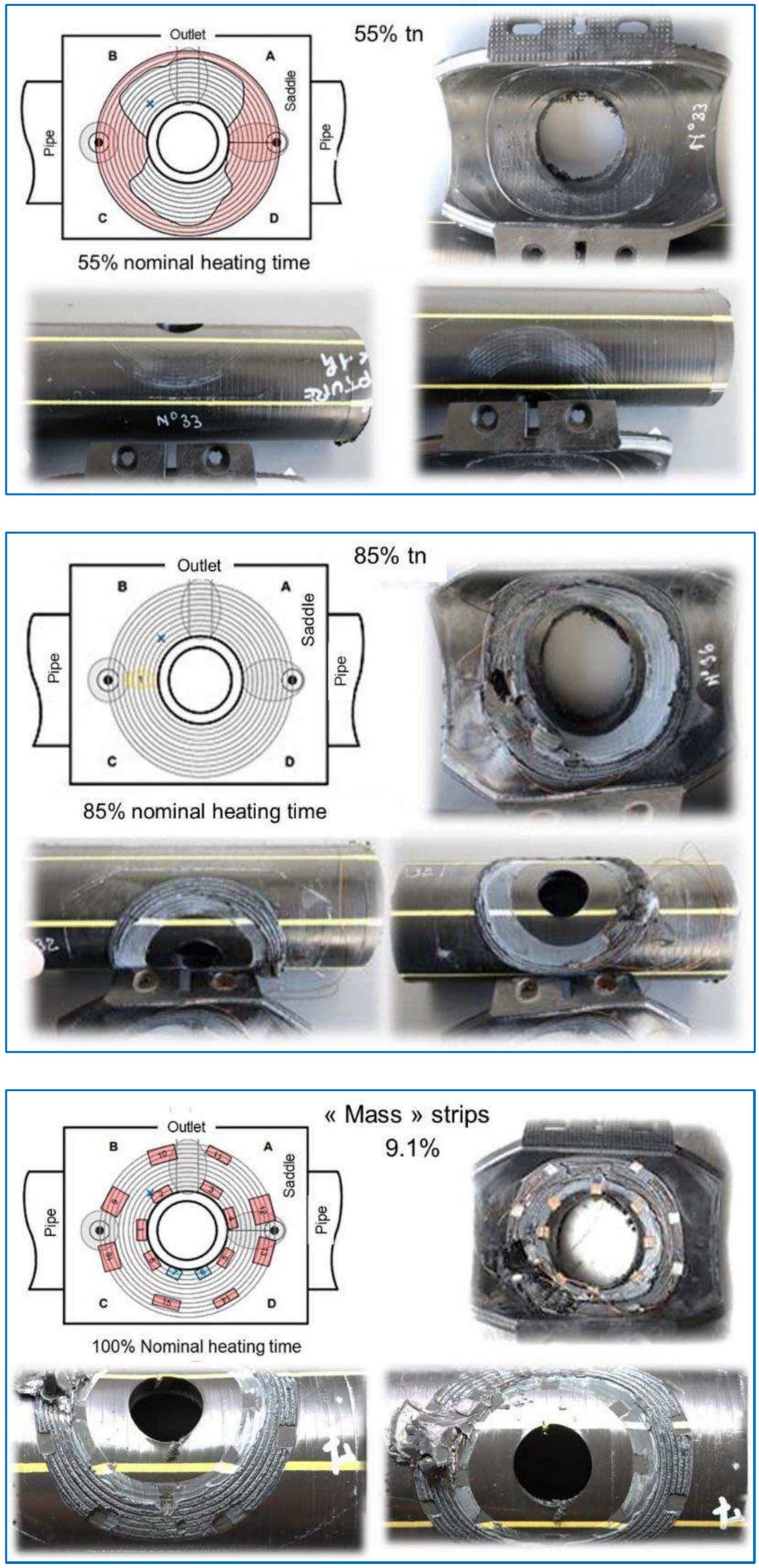

Fig. 25 continued

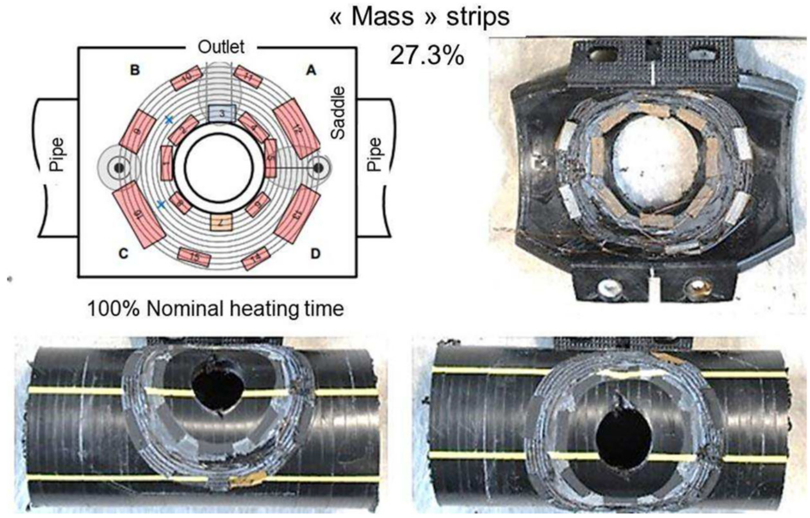

Comparison of the disorders on the assemblies with "mass" defects shows that for both ends of the spectrum in terms of the proportion of strips implanted in "mass" configuration, the PAUT technique detects unwelded zones surrounding the strips, just as is observed on the decohesion surfaces. The decohesion surface reveals a brittle zone, concentric to the saddle chimney and visually accounting for over 30% of the surface of the heating zone. This brittle zone seems to be initiated in the vicinity of the strips through coalescence. However, this comparison must be treated with caution in view of the geometry of this brittle zone which might correspond to the water exit pathway during the hydrostatic pressure test.

This analysis enlights the difficulty for correlating the proportion of the non-welded zones afterwards with the PAUT prior diagnosis, due to the disturbance created by the water exit pathway up to failure during HPT. Such comparisons between non-destructive and destructive tests must be done on specimens tested independently to avoid any disturbances.

5 Conclusions

To date, the test program carried out on a set of 72 electrowelded assemblies both pristine and with induced disorders shows that PAUT is very effective in catching and sizing both the Heat Affected Zone and the various disorders even very small, except in certain cases of inaccessibility of the ultrasonic transducer on the tapping saddle.

The hydrostatic pressure tests carried out on both the pristine and the faulty assemblies lead to results which comply with the NF EN 1555 standard minimum requirements even for high degrees of disorder violating the permitted values. The analysis of the peel test results carried out after hydrostatic pressure testing enlights the difficulty for correlating the proportion of the non-welded zones afterwards with the PAUT prior diagnosis, due to the disturbance created by the water exit pathway up to failure. Thus, all these results show the high degree of tolerance of the welded assemblies to these severe disorders and beyond, the high-levelled acceptance criteria associated.

These results, which show the high degree of tolerance to disorders exhibited by both tapping saddles and couplers, need to be completed and the acceptance criteria need to be redefined more accurately.

Moreover, the relevance of both the mechanical tests carried out to assess for weld quality and the standard requirements should be addressed more in-depth, to issue pertinent thresholds concerning the faulty assemblies.

Acknowledgements Gaz Réseaux Distribution France (GRDF) for their financial support

Author Contributions D. Gueugnaut and M. Tessier: co-writers M. Bechrouri and A. Lopitaux: Lab testing.

Funding This study was funded by Gaz Réseaux Distribution France Direction Technique et Industrielle (GRDF DTI).

Data Availability No datasets were generated or analysed during the current study.

Declarations

Competing Interests The authors declare no competing interests.

References

1. Hwang, J.S., Shin, H.J., Song, S.J., Song, T.K.: 26th review of progress in quantitative non-destructive evaluation. In: Thompson, D.O., Chimenti, D.E. (eds.) AIP Conference Proceedings, vol. 19A, 509, pp. 1087–1093 (1999)
2. Troughton, M.: Welding with integrated non-destructive examination of PE pipes. Plastics Pipes XI, München (Germany), 3-6 September 2001
3. Shin, H.J., Kwon, J.-R., Song, S.-J.: Ultrasonic real time imaging technique for the inspection of electrofusion joints for polyethylene piping. In: Korea Gas Safety Corporation (ed.) 2001 Forum for Gas Safety, KGS 2001-069, p. 21, 27 September 2001
4. Ghia, S., Olivero, D., Piovano, M.: Italgas experience on non-destructive evaluation of PE pipe welding. In: Proceedings of the Plastic Pipes XII, Milan, Italy, 19–22 April 2004
5. Shin, H.J., Jang, Y.H., Kwon, J.R., Lee E.J.: Non-destructive testing of fusion joints of polyethylene piping by real time ultrasonic imaging. In: Plastics Pipes XII Conference, Milan, Italy, 19–22 April 2004
6. Bird, C., Caravaca, D., Raude, A.: Plastics pipes XIII, "The Inspection of Cold Welds in Electrofusion Joints", session 7A, Washington DC, USA, 2-6t October 2006
7. Troughton, M., Brown, M., Hessel, J., Piovano, M.: Comparison of long-term and short-term tests for electrofusion joints in PE pipes. In: Proceedings of the Plastics Pipes XIII, Washington DC, USA, 2–5 October 2006
8. Gueugnaut, D., Garneret, G., Sèvre, B., Lopitaux, A.: Evaluation of the quality of the PE assemblies joined by electrofusion: analysis of the standardized tests designed to evaluate the cohesive resistance. In: 2008 International Gas Union Research Conference, Distribution Session N°199/E/S2, Cité des Sciences et de l'Industrie, Paris, France, 8–10 October 2008
9. Gueugnaut, D., Piovano, M., Garneret, G., Sèvre, B., Vacchina, M., Cantore C.: Evaluation of a new non-destructive technique of the polyethylene welded assemblies. In: 2008 International Gas Union Research Conference, Distribution Session N°196/E/S2, Cité des Sciences et de l'Industrie, Paris, France, 8–10 October 2008
10. Frederick, C.J.: Detection and quantification of detrimental conditions in HDPE using ultrasonic phased array. In: Proceedings of the Plastic Pipes XVI, Vancouver (BC), September 2010
11. Postma, P.J.: Suitable non-destructive testing techniques for polyethylene pipe joints. GERG PC Distribution Project n°GT-120214, October 2012
12. Postma P.: Plastic Pipes XVI, Barcelona, Spain, 24-26 September 2012
13. Troughton, M., Spicer, M., Hagglund, F.: Development of an automated phased array ultrasonic inspection system and flaw acceptance criteria for welded joints in polyethylene pipes. In: Proceedings of the Plastic Pipes XVI, Barcelona, Spain, 24-26 September 2012
14. Troughton, M., Jones, I., Andrews, S.: State of the art in welding thermoplastics and in assessing thermoplastic welded joints. Giornate Nazionali della Saldatura dei Materiali Plastici e Compositi, GNS7, Genoa (Italy), 23-24 May 2013
15. Troughton, M., Spicer, M., Hagglund, F.: Development and assessment of ultrasonic inspection system for polyethylene pipes. In: Proceedings of the ASME 2013 Pressure Vessels and Piping Conference, PVP2013, Paris, France, 14-18 July 2013
16. Hagglund, F., Robson, M., Troughton, M., Spicer, W., Pinson, I.: A novel phased array ultrasonic testing (PAUT) system for on-site inspection of welded joints in plastic pipes. In: 11th European Conference in Non-Destructive Testing (ECNDT), Prague, Czech Republic, October 2014
17. Troughton, M., Spicer, M., Hagglund, F.: Development and assessment of a phased array ultrasonic inspection system for polyethylene pipe joints. In: ANTEC 2014 Conference, Las Vegas, USA, April 2014
18. Seonghee, K., Jeongrock, K., Keebong, Y.: Proceedings of the 17th Plastic Pipes Conference, Chicago, Illinois, USA, 22-24 September 2014
19. Postma, P., Hermkens, R.: Suitability of non-destructive techniques for polyethylene pipe joints. A GERG investigation into the suitability of current techniques. Plastic Pipes XVII, Chicago, USA, 22-24 September 2014
20. ISO TC138/SC5 ISO/DTR16943: 2022. Thermoplastic pipes for the conveyance of fluids—inspection of polyethylene electrofusion socket joints using the phased array ultrasonic testing method
21. Gueugnaut, D., Boujlal, A., Sèvre, B., Angelini, F.: The capability of the ultrasonic phased array technique for detecting and measuring defects at the inner surface of a polyethylene pipe through an outside analysis. Plastic Pipes XVI, Barcelona, Spain, 24-26 September 2012
22. Gueugnaut, D., Boujlal, A., Bouaffre, R., Sèvre, B., Angelini, F., Louet, P.: Use of phased array technology for the inspection of polyethylene gas distribution pipes and fittings. In: European Symposium on Pressure Equipment ESOPE, Cité des Sciences de La Villette, Paris, 08-10 October 2013
23. Gueugnaut, D., Angelini, F., Boujlal, A., Bouaffre, R., Sèvre, B., Louet, P.: Ultrasonic phased array inspection of polyethylene pipelines & fittings used for gas distribution. Plastic Pipes XVII, Session 2B, Chicago, Illinois, USA, 22-24 September 2014
24. Gueugnaut, D., Angelini, F., Boujlal, A., Bouaffre, R., Sèvre, B., Louet, P.: 4th China International Plastic Pipe Conference, Shanghai, China, 21-22 September 2015

25. Gueugnaut, D., Tessier, M., Bouaffre, R., Lopitaux, A.: Ultrasonic phased array inspection of electrofused joints implemented in polyethylene gas piping systems. J. Mater. Sci. Eng. **7**(2), 68–81 (2017)
26. ISO 13956: 2010. Plastics pipes and fittings—decohesion test of polyethylene (PE) saddle fusion joints—evaluation of ductility of fusion joint interface by tear test
27. ISO 13954: 1997. Plastics pipes and fittings—peel decohesion test for polyethylene (PE) electrofusion assemblies of nominal outside diameter greater than or equal to 90 mm
28. ISO 13955: 1997. Plastics pipes and fittings—crushing decohesion test for polyethylene (PE) electrofusion assemblies
29. NF EN 1555-2: 2021. Plastics piping systems for the supply of gaseous fuels—polyethylene (PE)—part 2: pipes
30. NF EN 1555-3: 2021. Plastics piping systems for the supply of gaseous fuels—polyethylene (PE)—part 3: fittings
31. Troughton, M., Khamsehnzhad, A.: Development of flaw acceptance criteria for welded joints in PE pipes. ID25, p.71, NDT Workshop of Plastic Pipes XVIII, Berlin, Germany, 11-14 September 2016
32. Wermelinger, J., Hein, O.: Long term influence of defects in butt fusion joints on PE100 pipes and NDT detection of them. ID33, p.72, NDT Workshop of Plastic Pipes XVIII, Berlin, Germany, 11-14 September 2016
33. Gueugnaut, D., Bouaffre, R., Lopitaux, A., Renaud, R., Angelini, F., Louet, P.: Ultrasonic phased array evaluation of the integrity of polyethylene piping systems. In: 19th World Conference on Non-Destructive Testing, Münich (Germany), 13-17 June 2016
34. Gueugnaut, D., Angelini, F., Bouaffre, R., Tessier, M.: Ultrasonic phased array inspection of polyethylene damaged pipes with calibrated faults. ID96, p.67, NDT Workshop of Plastic Pipes XVIII, Berlin, Germany, 11-14 September 2016
35. Postma, P.: Determining acceptance criteria for non-destructive testing of electrofusion joints. ID181, p.73, NDT Workshop of Plastic Pipes XVIII, Berlin, Germany, 11-14 September 2016
36. Gueugnaut, D., Tessier, M., Bouaffre, R.: Acceptance criteria for volume defects in welded assemblies, detected and sized using the phased array ultrasonic technique. Plastic Pipes XIX, Session 4A, Las Vegas, NV, USA, 24-26 September 2018
37. Wermelinger, J., Choi, S.: Worldwide ISO Round Robin Study on phased array ultrasonic non-destructive test for electrofusion socket joints. In: Proceedings of the 20th Plastic Pipes Conference PPXX, Amsterdam, Netherlands, 6-8 September 2021
38. Gueugnaut, D., Wackernie, P., Forgerit, J.P.: Infrared microspectrometric study of the thermal history of fusion welding of polyethylene. J. Appl. Polym. Sci. **35**, 1683 (1988)
39. Berger, I.J., Frank, A., Pinter, G., Nitsche, D., Petry, D.: Investigation of the failure behavior of polyethylene electrofusion sockets. Plastic Pipes XIX, Session 4A, Las Vegas, NV, USA, 24-26 September 2018